Phosphorylation that Detaches Tau Protein from Microtubules (Ser262, Ser214) Also Protects It against Aggregation into Alzheimer Paired Helical Filaments†

A. Schneider, J. Biernat, M. von Bergen, E. Mandelkow, and E.-M. Mandelkow*

Max-Planck-Unit for Structural Molecular Biology, Notkestrasse 85, D-22603 Hamburg, Germany

Received August 5, 1998; Revised Manuscript Received October 26, 1998

ABSTRACT: One of the hallmarks of Alzheimer's disease is the abnormal state of the microtubule-associated protein tau in neurons. It is both highly phosphorylated and aggregated into paired helical filaments, and it is commonly assumed that the hyperphosphorylation of tau causes its detachment from microtubules and promotes its assembly into PHFs. We have studied the relationship between the phosphorylation of tau by several kinases (MARK, PKA, MAPK, GSK3) and its assembly into PHFs. The proline-directed kinases MAPK and GSK3 are known to phosphorylate most Ser-Pro or Thr-Pro motifs in the regions flanking the repeat domain of tau: they induce the reaction with several antibodies diagnostic of Alzheimer PHFs, but this type of phosphorylation has only a weak effect on tau−microtubule interactions and on PHF assembly. By contrast, MARK and PKA phosphorylate several sites within the repeats (notably the KXGS motifs including Ser262, Ser324, and Ser356, plus Ser320); in addition PKA phosphorylates some sites in the flanking domains, notably Ser214. This type of phosphorylation strongly reduces tau's affinity for microtubules, and at the same time inhibits tau's assembly into PHFs. Thus, contrary to expectations, the phosphorylation that detaches tau from microtubules does not prime it for PHF assembly, but rather inhibits it. Likewise, although the phosphorylation sites on Ser-Pro or Thr-Pro motifs are the most prominent ones on Alzheimer PHFs (by antibody labeling), they are only weakly inhibitory to PHF assembly. This implies that the hyperphosphorylation of tau in Alzheimer's disease is not directly responsible for the pathological aggregation into PHFs; on the contrary, phosphorylation protects tau against aggregation.

The brains of patients suffering from Alzheimer's disease are characterized by two types of abnormal protein deposits, amyloid plaques, and neurofibrillary tangles (NFT). Both consist of fibers of aggregated protein, the Aβ peptide in the case of plaques, and tau protein in the case of the tangles, neither of which is aggregated in its normal physiological state (*1*, *2*). The clinical progression of the disease correlates well with the neurofibrillary deposits; however, neuronal damage already occurs before fully developed tangles are observed (*3*, *4*). There is thus considerable interest in understanding the early steps of tau aggregation. Tau protein is a highly soluble protein that is normally attached to axonal microtubules, the tracks for axonal transport of vesicles and organelles. Tau protein is mainly found in the axons of neurons. It stabilizes microtubules and makes them rigid. The microtubule binding region of tau lies in the C-terminal half, including the 3 or 4 internal repeats. The basic and proline-rich regions flanking the repeats help to target tau to the microtubule, while the acidic N-terminus does not bind to the microtubule (*5*, *6*). The binding of tau to microtubules is regulated by (physiological) phosphorylation. Tau phosphorylated at certain sites can detach from microtubules so that they become more labile and dynamic. AD tau is "hyperphosphorylated" at a number of sites and does not bind to microtubules (*7*, *8*). This correlates with a loss of microtubules and the breakdown of axonal flow (*9*). At the same time the hyperphosphorylated tau is found aggregated into PHFs, despite tau's unusual solubility. To explain this, a common hypothesis holds that hyperphosphorylation changes tau's properties in some way (e.g., its conformation) so that aggregation into PHFs is promoted.

In principle this assumption could be tested by phosphorylating recombinant tau in vitro and observing its self-assembly into PHFs. Filament assembly studies have been successful with amyloid peptide in vitro (*10*), but in the case of tau such studies were hampered in several ways: (a) Tau can be phosphorylated by many kinases, at many sites, and with different effects on microtubule stabilization. Preparing sufficient amounts of different kinases, phosphorylating tau in a homogeneous manner, and ascertaining the state of phosphorylation can be a major problem. (b) The self-assembly of tau is exceedingly slow (days to weeks), and the assembly products can be heterogeneous. In vitro, PHF assembly can be promoted by several factors or conditions, for example, by using constructs containing only the repeats, oxidation of sulfhydrils (*11*, *12*), certain fatty acids (*13*), or anionic cofactors such as heparin, RNA, or acidic peptides (*14*−*18*). However, the role of these factors in vivo and the relationship between phosphorylation and PHF aggregation

† The project was supported by the Deutsche Forschungsgemeinschaft.

* Corresponding author. Tel: +49-40-89982810. Fax: +49-40-89716822. E-mail: mand@mpasmb.desy.de.

[1] Abbreviations: AD, Alzheimer's disease; CaMK, Ca++, calmodulin-dependent kinase; cdk5, neuronal cdc2-like kinase; GSK-3, glycogen synthase kinase-3; MAPK, mitogen activated protein kinase; MARK, microtubule affinity regulating kinase; NFT, neurofibrillary tangles; PHF, paired helical filaments; PKA, protein kinase A, cAMP-dependent kinase.

10.1021/bi981874p CCC: $18.00
Published on Web 03/06/1999

remained elusive.

Kinases affecting tau's phosphorylation have been studied mainly from two angles: their effect on tau-microtubule interactions, and their effect on Alzheimer-like hyperphosphorylation. A number of monoclonal antibodies have been generated which detect the AD-like state of tau, and many of these have epitopes containing phosphorylated SP or TP motifs (for reviews, see refs *19*−*21*). This points to an involvement of proline-directed kinases, for example, MAP kinase, GSK3, or cdk5. Although these kinases can phosphorylate tau at many sites (thereby inducing a reaction with Alzheimer diagnostic antibodies), their effect on microtubule interactions is only moderate. By contrast, other non-proline-directed kinases can inhibit tau−microtubule binding strongly by phosphorylating certain sites, for example, S262 (by the kinase MARK) or S214 (by PKA) (*22*−*26*). In this study we have therefore chosen two kinases from each class, the proline-directed kinases MAPK and GSK-3 versus the non-proline-directed kinases MARK and PKA, and studied their effect on tau phosphorylation and PHF assembly.

Following the initial hypothesis, we had expected that one of the modes of phosphorylation would promote PHF assembly. However, the results revealed the opposite: Phosphorylation never enhanced aggregation; on the contrary it protected against it. Thus, the effects of tau phosphorylation on microtubule interactions parallel the effects on PHF assembly, that is, the same phosphorylation that prevents tau's binding to microtubules also protects it against PHF assembly.

MATERIALS AND METHODS

Cloning and Preparation of Recombinant Tau Protein. Constructs of tau (Figure 1) were designed and expressed in *Escherichia coli* BL21(DE3) strain as described (*22*). The numbering of the amino acids used here refers to the isoform tau40 containing 441 residues (*27*). The isoform Tau23 is the shortest one in human CNS; compared to tau40 it lacks the second repeat and the near-N-terminal inserts. K19 contains only the repeats. AP25 is derived from Tau23, except that 10 SP or TP motivs are changed into AP, leaving only four such motifs at T111, T217, T231, and S235. The expressed proteins were purified from bacterial extracts making use of the heat stability and following FPLC Mono S (Pharmacia) chromatography (*22*). The purity of the proteins was analyzed by SDS−PAGE.

PHF Formation. Tau or tau constructs were incubated at concentrations of 80 or 100 μM in 10 mM MOPS, pH 7.0, and a cocktail of protease inhibitors at 37 °C. As cofactors of polymerization we used polyanions such as RNA, poly-Glu, or heparin (20 or 25 μM, see ref *18*). The incubation time varied between 1 h and 14 days. PHF formation was checked by electron microscopy and Thioflavine S fluorescence (*18*) and quantified by gel assay.

Quantification of PHF Assembly. PHFs were centrifuged with 100000*g* for 1 h at 4 °C. The PHF pellet was washed twice with 10 mM ammonium acetate. The resulting pellets and supernatants were dried and resuspended in sample buffer containing 5% β-mercaptoethanol. Pellets and supernatants were boiled at 95 °C for 5 min to dissolve PHFs and subjected to SDS−PAGE (10% or 15% acrylamide). Gels were stained with Coomassie brilliant blue R250. The stain intensity was calibrated against concentration series of bovine serum albumin and Tau23. For quantification of protein amounts the gels were scanned using a HP ScanJet 4C scanner. For quantification of radioactivity Image Plates were exposed and scanned with a Bas2000 Phosphoimager (Raytest, Straubenhardt, Germany). Evaluation was done using the program TINA 2.0 (Raytest). Experiments were usually evaluated as part of a time series to determine the increase in PHF formation (up to 14 days) and were reproducible to within ~10−20%.

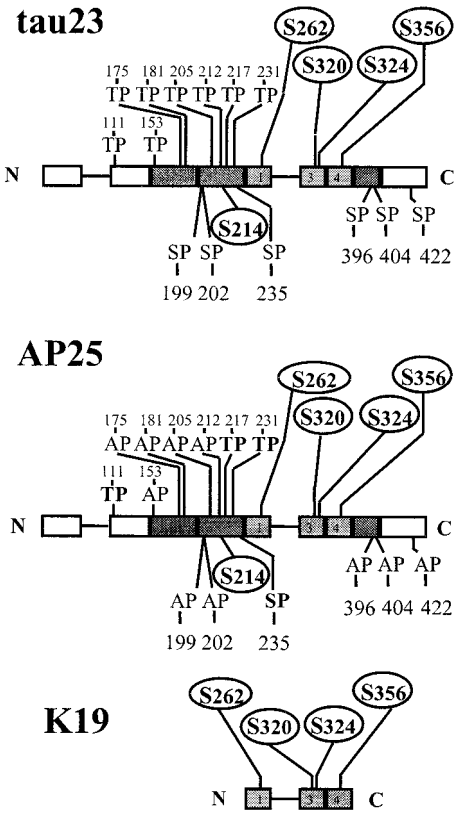

FIGURE 1: Tau constructs and phosphorylation mutants. Top: Bar diagram of human Tau23, the smallest isoform (352 residues). The second repeat (R2) and the two inserts near the N-terminus are absent due to alternative splicing. The numbering of residues follows that of Tau40, the largest isoform in the CNS (441 residues, ref *27*). Some of the potential phosphorylation sites are indicated: the 14 SP or TP motifs are targets of proline-directed kinases, the KXGS motifs in each repeat are targets of MARK or PKA (circled), and additional targets of PKA are S320, S214, T245. Middle: The construct AP25 is derived from Tau23, but 10 of the 14 SP or TP motifs are mutated into Ala (A153, A175, A181, A199, A202, A205, A212, A396, A404, A422) making them nonphosphorylatable, while 4 are retained (T111, T217, T231, S235). Bottom: The construct K19 contains only the three repeats. There are no SP or TP motifs but three KXGS motifs, one in each repeat (containing S262, S324, S356), and S320, all phosphorylatable by MARK or PKA.

Electron Microscopy. Protein solutions were diluted to about 5−10 μM protein and placed on 600-mesh carbon-coated copper grids for 1 min and negatively stained with 2% uranyl acetate for 45 s. Specimens were examined in a Philips CM12 electron microscope at 100 kV.

Protein Kinases. Recombinant MEK (MAP kinase activator) was prepared by K. Stamer, recombinant MAPK by S. Illenberger, recombinant GSK-3β by R. Godemann, and recombinant MARK by G. Schmidt-Ulms. The cAMP-dependent protein kinase catalytic subunit (PKA) was

obtained from Promega (Madison, Wisconsin).

Phosphorylation Reactions. The phosphorylation of tau by MARK, PKA, MAP kinase, or GSK-3β was carried out at 37 °C in 40 mM Hepes, pH 7.2, 3 mM $MgCl_2$, 5 mM EGTA, 1 mM PMSF, 2 mM [γ-^{32}P]ATP (100−200 Ci/mol, Amersham), and a cocktail of protease inhibitors (leupeptin, aprotinin, pepstatin A at 10 μg/μL each and 1 mM PMSF). Conditions were varied in order to achieve the phosphorylation at certain types of sites; in most cases this includes the use of heparin which enhances the efficiency of phosphorylation and modifies the pattern as well (*28*, *29*). Phosphorylation reactions were carried out for various time periods (∼15 min to 16 h) and terminated by brief heating to 95 °C. The extent of phosphorylation was assayed from the radioactivity in SDS gels. The protein fraction used for PHF assembly assays was boiled in 0.5 M NaCl, 5 mM DTT, for 5 min. The heat-denatured kinase was pelleted by centrifugation, and supernatants containing the heat-stable soluble tau were brought into 10 mM NH_4-acetate using a NAP-5 gel filtration column (Pharmacia) or a PC3.2/10 fast desalting column (Smart System, Pharmacia) (this step served to remove the DTT which otherwise would inhibit dimerization of tau and PHF assembly). The samples were then lyophilized (Speedvac SC110, Bachhofer, Reutlingen) and resuspended in 10 mM MOPS, pH 7, and a cocktail of protease inhibitors. Protein concentrations were determined by SDS gel assay (see above). Control experiments without the boiling step showed that boiling per se had no influence on the kinetics or appearance of PHFs.

Phosphorylation of Synthetic Filaments. Synthetic filaments were separated from unpolymerized protein by centrifugation (1 h, 100000*g*). Filaments were lyophilized, resuspended in 10 mM NH_4Ac, and checked by electron microscopy. Phosphorylation reaction was done in phosphorylation buffer without DTT but with heparin at filament concentrations between 0.25 and 1 μg/μL for 5−16 h at 37 °C. The sample was centrifuged for 1 h at 100000*g* and washed twice with 10 mM NH_4Ac to separate filaments from dissociated protein. The phosphate content was determined, and the pellet was checked for filaments by electron microscopy before 2D phosphopeptide analysis was done.

Phosphopeptide Mapping. Following phosphorylation reactions, the kinase was removed by boiling in 0.5 M NaCl, 5 mM DTT and centrifugation. The heat-stable tau protein was precipitated by 15% trichloroacetic acid. Cysteine residues were oxidized by performic acid treatment, and the protein was digested overnight with trypsin (Promega, sequencing grade) using two additions of enzyme in a ratio of 1:20 (w/w). Two-dimensional phosphopeptide mapping by thin-layer electrophoresis/chromatography was performed on thin-layer cellulose plates (Macherey & Nagel, Düren, Germany) according to ref 30.

Identification of Phosphopeptides. The phosphopeptides were eluted and purified by rpHPLC as described (*24*, *31*). Spots were identified by double runs with known peptides and analyzed using a 476A Liquid-Phase Protein Sequencer (Applied Biosystems) and MALDI-MS (matrix-assisted laser desorption ionization mass spectroscopy, Shimadzu MALDI II).

Immunoblots. The proteins were transferred to PVDF membranes (Millipore, Eschborn, Germany), and residual protein binding sites were blocked with 5% milk powder in TBS−Tween buffer. The blots were incubated for 1 h at 37 °C with 12E8 (1:5000), washed, and incubated with horseradish peroxidase conjugated secondary antibody for 1 h at room temperature. After washing, bound antibodies were detected by the ECL System (Amersham, Braunschweig, Germany).

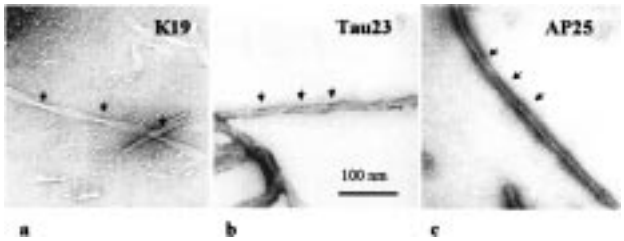

FIGURE 2: Electron micrographs of PHFs assembled in vitro from different tau constructs: (a) K19, (b) Tau23, and **(c)** AP25. Protein concentrations were 100 μM. Assembly was done at 37 °C for several days in the presence of 25 μM heparin (*14*). Note that all three proteins form filaments similar to Alzheimer PHFs (crossover repeat about 80 nm, width 10−20 nm). Bar = 100 nm.

RESULTS

(a) Assembly of Tau into PHFs Is Inhibited by Phosphorylation with MARK and PKA. The tau constructs used in this study were derived from the isoform Tau23, the smallest in the human CNS (Figure 1). The choice was based on the following rationale: Since the second repeat is absent in the constructs they contain only a single cysteine, C322. This facilitates the formation of tau dimers by disulfide bridging, and hence the assembly of PHFs in vitro, because tau dimers act as the effective building blocks (*11*). The construct K19 was chosen because the core of Alzheimer PHFs is largely made up of the repeats (*32*), and because the repeats aggregate most efficiently into PHFs in vitro (*12*, *16*). By contrast, the nonrepeat domains, especially the N-terminal projection domain, act as inhibitors of PHF assembly, so that full-length tau hardly assembles at all, except in the presence of exogenous catalysts such as heparin, RNA, or poly-Glu (*14*−*18*). Third, the mutant AP25 was designed in order to eliminate most of the potential phosphorylation sites by proline-directed kinases such as MAP kinase, GSK-3, or cdk5.

The constructs shown in Figure 1 readily form PHFs when they are allowed to dimerize and are stimulated to assemble by polyanions (Figure 2). The extent of PHF assembly can be assayed by a fluorescence assay (*18*), or by quantitating the supernatant and pellet after centrifugation, as in this study (see Methods). Since the "abnormal" phosphorylation of tau is an early step in the neuritic pathology (*32*, *33*), we anticipated that this phosphorylation would detach tau from microtubules and subsequently facilitate PHF assembly. However, when Tau23 is phosphorylated by MARK or PKA, the extent of PHF assembly is strongly inhibited (Figure 3a,b). By contrast, proline-directed kinases (MAP kinase, GSK-3β) induce only a weak inhibition (Figure 4a). These classes of kinases affect different phosphorylation sites, as shown by the phosphopeptide maps (Figures 3, 4; for analysis of peptides see refs *26*, *31*, and *35*). The major sites targeted by MARK are the KXGS motifs in repeats R1 (S262), R3 (S324), and R4 (S356), plus S320 in repeat R3 (Figure 3c). PKA (stimulated with heparin) phosphorylates the same sites,

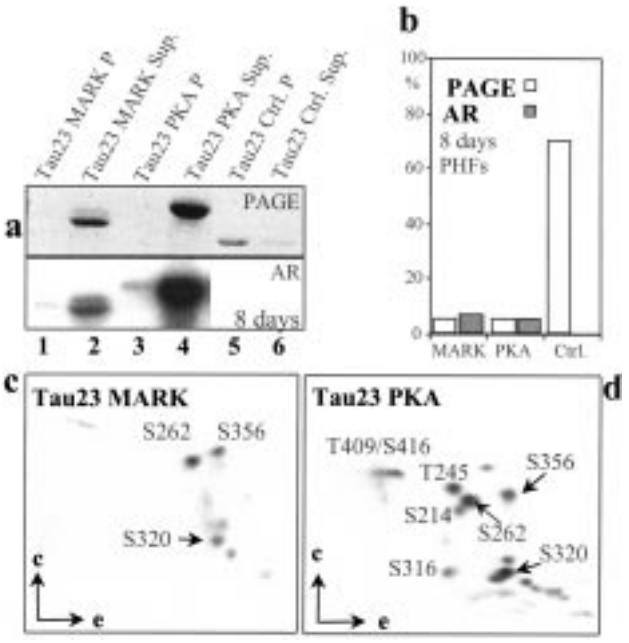

FIGURE 3: Phosphorylation of Tau23 with MARK or PKA and effect on PHF assembly. (a) Top: SDS gel of Tau23 phosphorylated with MARK (lanes 1, 2), PKA (lanes 3, 4), and unphosphorylated control (lanes 5, 6), assembled into PHFs (8 days), and separated into pellet (P, lanes 1, 3, 5) and supernatant (Sup, lanes 2, 4, 6). Bottom: Autoradiography showing that the phosphorylated protein remained largely in the supernatant (lanes 2, 4). (b) Extent of PHF assembly (8 days) of unphosphorylated Tau23 (control, right), or after phosphorylation with MARK (16 h, left) or PKA (16 h, center). The assembly was determined by sedimentation of the polymer and quantification by SDS−PAGE (white bars) or autoradiography (shaded bars) and given in relative units (total protein = 100%). Protein found in the pellet represents the amount of filaments. Protein, which has not assembled into filaments, remains in the supernatant. The extent of filament assembly is shown in the percent of total protein, that is, the protein amount assembled into filaments plus the amount of protein which has not formed filaments. Therefore quantification is independent from absolute protein amounts subjected to the gel. Note the nearly complete inhibition of PHF assembly by phosphorylation. (c, d) 2D phosphopeptide maps of Tau23 phosphorylated with MARK (c) or PKA (d). The phosphorylation conditions were the same as in Figure 3a. In (c) the main phosphorylation sites induced by MARK are S262 and S356 (in the KXGS motifs of repeats R1 and R4) followed by S320; there are no major sites outside the repeats. The total extent of phosphorylation was 2.6 mol of Pi/mol of Tau. In (d) the prominent sites phosphorylated by PKA are S262, S320, and S356 in the repeats (similar as with construct K19, see Figure 7c below); additional pronounced sites are S214 and T245. The total extent of phosphorylation is 3.9 mol of Pi/mol of Tau.

and in addition T245, S409, and S416 (Figure 3d), but the most pronounced initial PKA site is S214 in the P-domain upstream of the repeats. Thus, a few critical sites in the repeats are already sufficient to prevent PHF assembly. Since the phosphorylation of KXGS motifs also leads to the dissociation of tau or other MAPs from microtubules (e.g., at S262, refs *23*, *31*), we can conclude that the same type of phosphorylation that dissociates tau from microtubules protects tau from polymerizing into PHFs.

In contrast, the proline-directed kinases GSK-3β and MAPK have only a weak effect on PHF assembly. As expected from their substrate specificity, the sites are restricted to SP or TP motifs, most of which lie in the domains flanking the repeats on either side (Figure 4b,c; for details on the analysis see refs *24*, *36*). Because of the number of such motifs (14 in Tau23), the phosphopeptide pattern is more complex than that of MARK or PKA, but the important point is that even collectively these sites are not nearly as efficient in suppressing PHF assembly. This finding parallels the effect of proline-directed kinases on tau−microtubule interactions which is also weak (*22*). We conclude that phosphorylated SP or TP motifs have only a mild effect on tau−tubulin and tau−tau interactions, even though these motifs dominate the abnormal phosphorylation of tau and the reactions with Alzheimer-diagnostic antibodies.

(b) Phosphorylation of the Single-Site S214 by PKA Protects Tau Against PHF Assembly. MARK and PKA show similar phosphorylation sites within the repeat domain (Figure 3c,d), suggesting that these sites are the critical ones for PHF assembly. In addition PKA phosphorylates targets outside of the repeat domain, leaving the possibility that these could also affect PHF assembly. The site at S214 is particularly interesting because it forms part of a unique epitope of the antibody AT100 specific for Alzheimer tau (*36*, *37*), is enhanced in mitotic cells, and is capable of detaching tau from microtubules (*24*). We therefore asked whether this site would also have an effect on PHF assembly (Figure 5). The role of S214 can be studied selectively because it is highly reactive with PKA so that short incubation times generate only this single phosphorylated residue (Figure 5b). Surprisingly, this single site also inhibits PHF assembly almost completely (Figure 5a).

The experimental conditions allow us to address issues of the assembly pathway: As shown earlier, the efficiency of PHF formation strongly depends on tau dimers linked by a disulfide bridge at C322 (*12*). Phosphorylation at S214 might therefore inhibit either the initial dimerization or some later step. Figure 5c shows that the time course of dimerization is independent of phosphorylation at S214. This means that the inhibition of PHF assembly occurs at a stage after dimerization, for example, nucleation or elongation of PHFs. In contrast, the phosphorylation of the KXGS motifs inhibits already the dimerization of tau (Figure 5d), most noticeably when S320 is phosphorylated as well.

As S214 lies in the flanking region rich in SP and TP motifs, we wanted to know whether neighboring sites had an effect as well. The most reactive target of Tau23 for MAP kinase is S235 so that short incubation times (~1 h) lead to 80% phosphorylation at that site (Figure 6b). However, there is no noticeable inhibition of PHF assembly (Figure 6a,c). Similarly, the mutant AP25 contains four SP or TP motifs (T111, T217, T231, S235), of which T217 is by far the most reactive for GSK-3β (Figure 6e). This site also has no inhibitory effect on PHF assembly (Figure 6d,f), in contrast to the adjacent PKA site S214.

(c) Phosphorylation of the Repeat Domain at KXGS Motifs and at S320 Inhibits PHF Assembly. Since the repeat domain forms the backbone of PHFs in Alzheimer brains, we wanted to analyze its dependence on phosphorylation separately from the projection and C-terminal domains. We therefore studied construct K19 which contains the three repeats R1, R3, and R4 only. K19 forms dimers, assembles into PHFs (*11*, *16*), and is amenable to selective phosphorylation since it contains only a few potential sites (and no SP or TP motifs). Phosphorylation of K19 with MARK or PKA inhibits PHF formation, but the effect is not as pronounced as with full-length tau (Figure 7). The prominent sites in K19 are similar

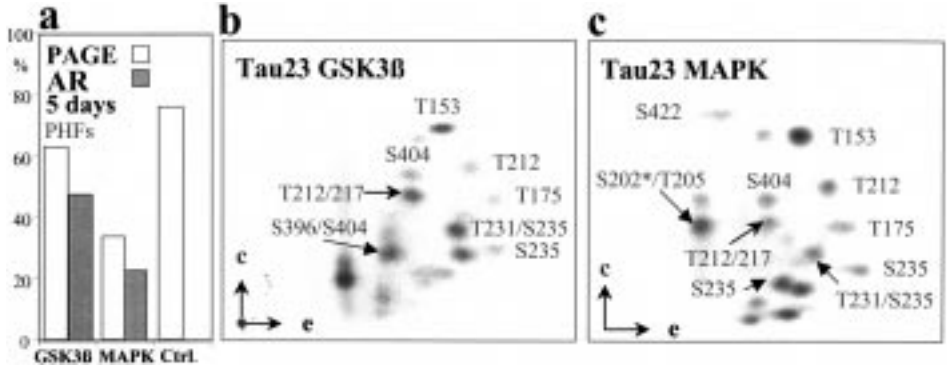

FIGURE 4: Phosphorylation of Tau23 with GSK-3β or MAPK has only a minor effect on PHF assembly. (a) Extent of PHF assembly (5 days) of unphosphorylated Tau23 (control, right), or after phosphorylation with GSK3β (16 h, left) or MAPK (16 h, center). The assembly was determined by sedimentation of the polymer and quantification by SDS−PAGE (white bars) or autoradiography (shaded) and given in relative units (total protein = 100%). Note that there is only partial inhibition of PHF assembly by phosphorylation at SP or TP sites. (b, c) 2D phosphopeptide maps of Tau23 phosphorylated with GSK-3β (b) or MAPK (c). The phosphorylation conditions were the same as in Figure 4a. In (b) the phosphorylation by GSK-3β is distributed over 7 major and 4 minor sites, mostly in the regions flanking the repeats (for details, see refs *36*, *26*). The total extent of phosphorylation was 2.8 mol of Pi/mol of Tau. In (c) the phosphorylation by MAPK is distributed over 6 major and 10 minor sites in the flanking regions. The total extent of phosphorylation is 4.7 mol of Pi/mol of Tau.

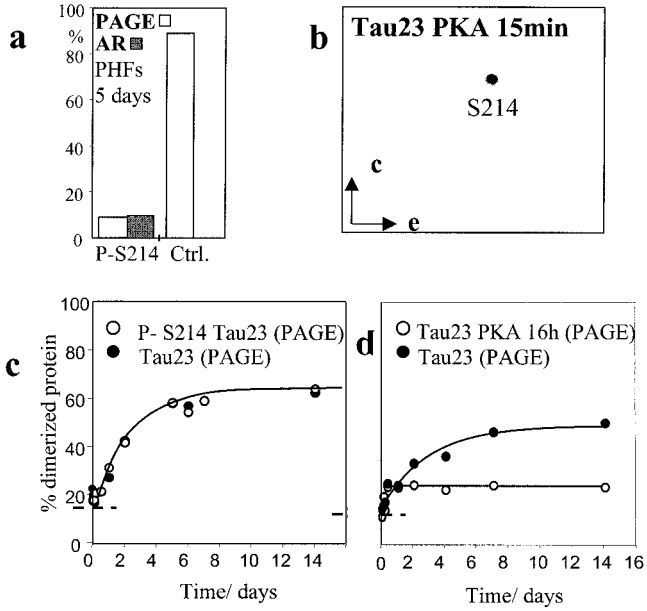

FIGURE 5: Phosphorylation of S214 by PKA blocks PHF assembly, but not dimerization of Tau23, whereas phosphorylation in the repeats inhibits dimerization and assembly. (a) Extent of PHF assembly (5 days) of unphosphorylated Tau23 (control, right), or after brief phosphorylation with PKA (15 min, left) so that only S214 becomes phosphorylated (see b). SDS−PAGE (white bars) and autoradiography (shaded) of assembled PHFs. Note the strong inhibition of PHF assembly by phosphorylation at S214. (b) 2D phosphopeptide map of Tau23 phosphorylated with PKA for 15 min, showing only a single phosphopeptide containing S214. The total extent of phosphorylation was 1.1 mol of Pi/mol of Tau. (c) Dimerization of Tau23 by disulfide cross-linking at C322 after brief (15 min) phosphorylation by PKA (open circles), or unphosphorylated control (filled circles). The two reaction curves are superimposable, showing that the phosphorylation does not prevent dimerization, even though it inhibits a later step of PHF assembly (see panel a). The initial level of ~15% dimers results from the preceding lyophilization in the absence of DTT. For details on dimerization, see ref 12. (d) Experiment similar to (c) but now after extensive phosphorylation of Tau23 with PKA (16 h, 20 μM heparin, open circles), or unphosphorylated control (filled circles). The additional phosphorylation in the repeats inhibits dimerization of tau by ~60%. For phosphopeptide map see Figure 3d.

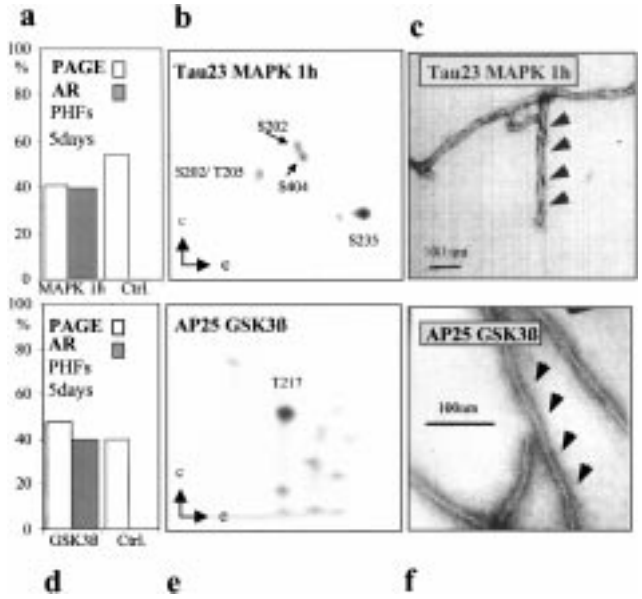

FIGURE 6: "Single-site" phosphorylation of S235 by MAPK or T217 by GSK-3β does not inhibit PHF assembly. (a) Extent of PHF assembly (5 days) of unphosphorylated Tau23 (control, right), or after brief phosphorylation with MAPK (1 h, with 20 μM heparin, left) so that S235 is the major phosphorylation site (see panel b). SDS−PAGE (white bars) and autoradiography of assembled PHFs (shaded). There is only a weak inhibition of PHF assembly by phosphorylation. (b) 2D phosphopeptide map of Tau23 phosphorylated with MAPK for 1 h, showing the major phosphorylation site (80%) at S235 and minor ones at S202, S404, and doubly phosphorylated S202/T205 (26). The total extent of phosphorylation was 1.0 mol of Pi/mol of Tau. (c) Electron micrograph of PHFs formed from Tau23 phosphorylated by MAP kinase, showing the normal twisted appearance. Bar = 100 nm. (d) Extent of PHF assembly (5 days) of unphosphorylated AP25 (control, right), or after phosphorylation with GSK-3β (16 h with 20 μM heparin, center) so that T217 is the major phosphorylation site (see panel e). SDS−PAGE (white bars) and autoradiography of assembled PHFs (shaded). There is no inhibition of PHF assembly by phosphorylation. **(e)** 2D phosphopeptide map of AP25 phosphorylated with GSK-3β for 16 h, showing the major phosphorylation site (95%) at T217. The total extent of phosphorylation was 0.8 mol of Pi/mol of Tau. (f) Electron micrograph of PHFs formed from construct AP25 phosphorylated with GSK-3β, showing the normal twisted appearance. Bar = 100 nm.

as with Tau23 (Figure 7c,d). MARK phosphorylates the two KIGS motifs in repeats R1 and R4 (S262 and S356, ~40% each, Figure 7b), followed by S324 in the KCGS motif of repeat R3 (~20%). In the case of PKA a further prominent site is S320 (Figure 7d) which may account for the stronger

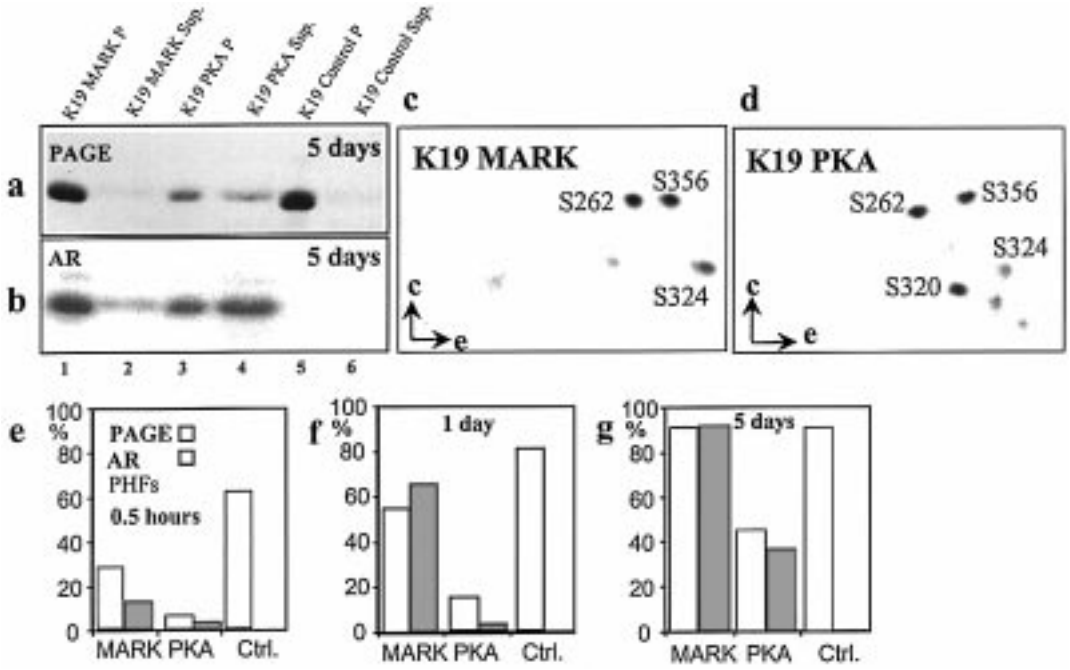

FIGURE 7: Inhibition of assembly of the repeat domain K19 into PHFs after phosphorylation with MARK or PKA. (a) Extent of PHF assembly of contruct K19 after phosphorylation (16 h, 20 μM heparin) by MARK (lanes 1, 2) or PKA (lanes 3, 4). Lanes 5 and 6 show the unphosphorylated control. Pellets of assembled PHFs (P, lanes 1, 3, 5) and supernatants (Sup, lanes 2, 4, 6). (b, c) Phosphopeptide maps of K19 phosphorylated with MARK or PKA. (b) The two most prominent phosphorylation sites generated by MARK are S262 and S356 (in the KXGS motifs of repeats no. 1 and 4), followed by S324 (KXGS motif in repeat no. 3). (c) The main sites generated by PKA are S262, S356, S324 (less pronounced), and S320 (not in a KXGS motif). The total extent of phosphorylation was 1.0 and 1.5 mol of Pi/mol of Tau for MARK and PKA, respectively. **(e, f, g)** Time course of PHF assembly (0.5 h, 1 day, 5 days). White bars show extent of polymerized K19 (pellet) as fraction of total protein, and shaded bars show fraction of total radioactivity in the pellet. Note the slower assembly of phosphorylated K19 compared with control (bar on right) and the delayed incorporation of phosphorylated protein into PHFs, most pronounced at early times (shaded bars), indicating that the initial stages of PHF assembly are particularly sensitive to phosphorylation.

inhibition of PHF assembly. This would be understandable considering that S320 and S324 sandwich the C322 which is important for the dimerization of tau. In summary, three or four phosphorylation sites in the repeats can slow the assembly of the repeat domain and almost completely block the assembly of full-length tau (cf. Figure 3). Although the initial rate of filament assembly is reduced after phosphorylation, particularly with PKA (Figure 7e,f,g), the final extent becomes comparable. This is confirmed by the fraction of radioactive Pi incorporated into the PHFs. At early times, incorporation of phosphate is very low, implying that the bulk of assembly occurs initially from unphosphorylated protein, but later the phosphorylated molecules become incorporated as well (Figure 7e,f,g).

(d) Many Phosphorylation Sites Remain Accessible Even after PHFs Have Been Formed. Thus far we have shown that a combination of certain phosphorylation sites, for example, S214, S262, S320, S324, or S356, can protect tau against PHF aggregation; some of these also efficiently interrupt the interaction with microtubules (S262, S214). On the other hand, in PHFs from AD tissue some of these sites are highly phosphorylated (*8*, *38*). To resolve this contradiction we asked whether PHFs, once formed, can still be phosphorylated. Figure 8a shows the example of Tau23 first assembled into PHFs and then phosphorylated with MAP kinase. The overall extent of phosphorylation is only ~30% of the unassembled protein, but even in the polymerized state many SP or TP sites are still exposed and available for phosphorylation. This agrees with the fact that these sites have little influence on PHF assembly (Figure 4), and that the proline-rich domain is largely part of the "fuzzy coat" of PHFs but not of the core (*32*, *39*). This would also be one explanation why antibodies against phosphorylated SP or TP motifs react with Alzheimer PHFs.

By contrast, Figure 8b illustrates a result that appears to be counterintuitive: Even sites whose phosphorylation blocks the assembly of Tau23 into PHFs are accessible for phosphorylation after PHFs are formed. This includes the sites S262 and S356 (targets of MARK or PKA) and S214 (PKA). A similar result applies to the repeat domain K19 whose post-assembly phosphorylation by MARK results in two prominent spots at S262 and S356 (Figure 8c). The post-assembly phosphorylation has no noticeable effect on the appearance of the PHFs (Figure 8d). The phosphorylation of S262 and S365 can also be detected by immunoblotting with antibody 12E8 (*40*), illustrating that the sites are indeed generated after polymerization of K19 (Figure 8e). The result is consistent with the mass spectroscopy data showing that S214, S262, and others are prominent phosphorylation sites in Alzheimer PHFs (*8*), and that the epitope of the Alzheimer-specific antibody AT100 includes phosphorylated S214 (*36*, *37*).

DISCUSSION

(a) "Hyperphosphorylation" Protects Tau against Assembly into Paired Helical Filaments. Aggregated tau protein in the form of PHFs is one of the hallmarks of Alzheimer's disease; it correlates with the progression of the disease (*3*, *4*) and is considered to be detrimental to the neurons because the protein becomes dislocated from the axonal into the somatodendritic compartment, obstructs intracellular traf-

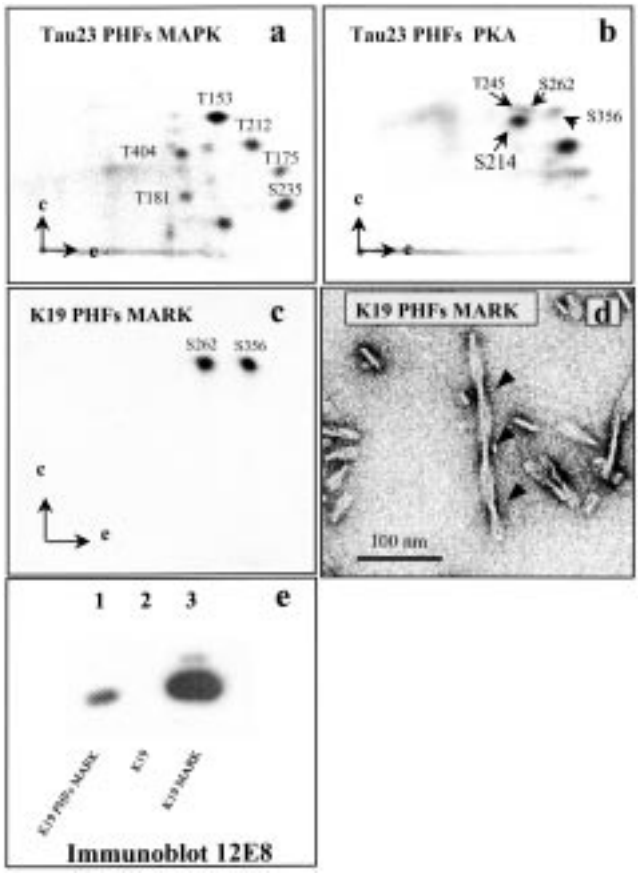

FIGURE 8: Accessibility of phosphorylation sites after assembly of PHFs. (a) 2D phosphopeptide map of Tau23 first assembled into PHFs (5 days, 20 μM heparin), then phosphorylated with MAPK (16 h, 20 μM heparin). Note that many SP or TP motifs are still accessible, especially those in the proline-rich domain preceding the repeats (T153, T175, T212, S235). (b) Phosphopeptide map of Tau23 first assembled into PHFs (5 days, 20 μM heparin), then phosphorylated with PKA (16 h, 20 μM heparin). The sites S214, T245, S262, and S356 are phosphorylated, whereas the sites S320 and S324 are not visible. Note that a fraction of the sites that would be inhibitory for tau's assembly into PHFs can still be phosphorylated after PHF assembly is completed, that is, S262, S356, and S214. The extent of phosphate incorporation is ~30% of that expected for phosphorylation of unpolymerized Tau. (c) Phosphopeptide map of K19 first assembled into PHFs (2 days), then phosphorylated with MARK (5 h, 20 μM heparin**)**. S262 and S356 are still prominent phosphorylation sites, but S320 is not (compare Figure 7c). (d) Electron micrograph of PHFs assembled from K19 and then phosphorylated with MARK, showing the typical twisted appearance of PHFs. Bar = 100 nm. (e) Immunoblot of K19 with antibody 12E8 recognizing phosphorylated S262 and S356 (40): center, unphosphorylated K19; right, K19 phosphorylated with MARK without assembly; and left, K19 first assembled into PHFs, then post-phosphorylated with MARK.

ficking, and no longer binds and stabilizes microtubules, the tracks for axonal transport (for reviews see refs *19*, *42*, *43*). Tau is abnormally elevated in the cerebrospinal fluid of Alzheimer patients and thus provides a potential tool for early diagnosis (*44*). Tau is necessary for neurite outgrowth and maintenance, and suppression of tau synthesis causes retraction and decay of neurites reminiscent of the decay in AD (*45*, *46*). On the other hand tau serves as a regulator of intracellular traffic in neurons and in particular affects kinesin-dependent transport along microtubules (*47*). These observations provide the justification for studying the molecular and cell biological functions of tau protein.

In AD, tau is more highly phosphorylated than normal adult tau (~8 vs ~2 Pi/molecule, ref *48*), there are more phosphorylation sites (*8*), and phosphorylation precedes PHF aggregation (*33*). The AD-like phosphorylation is particularly evident on SP or TP motifs in the domains flanking the repeats. These are phosphorylated by proline-directed kinases (e.g., MAP kinase, GSK3β, cdk5) and are recognized by a number of antibodies which are therefore useful as diagnostic reagents (*21*). In addition, AD tau shows enhanced phosphorylation at sites targetted by other kinases, for example, S262 in the first repeat (phosphorylated most efficiently by MARK, but also by PKA) or S214 (a target of PKA). The origin of the enhanced phosphorylation is a matter of debate; it could be due to an over-activity of kinases or an under-activity of phosphatases (*49*). In either case the initial cause could be a misregulation of some signal transduction cascade, possibly triggered by a toxic challenge, which affects the interplay between cellular kinases and phosphatases.

Tau is one of the most soluble proteins known (*50*, *51*), and therefore its aggregation in AD is particularly enigmatic. In vitro studies have shown that the repeat domain can be induced to form PHFs, albeit with low efficiency (*11*). By contrast, PHF assembly from full-length tau requires stimulation with polyanionic factors such as heparin, RNA, or poly-Glu (*14*−*16*). This argues that the regions outside the repeats are inhibitory for PHF assembly, consistent with the observation that the core of PHFs contains mainly the repeat domain, while the other domains contribute to the "fuzzy coat" which can be cleaved off by proteases (*32*, *52*).

Given these features of PHFs in AD, a widely accepted hypothesis can be summarized as follows (for review, see ref e.g. *42*): Due to some challenge (e.g., stress, amyloid peptide, etc.), the balance of kinases and phosphatases could be perturbed in neurons, causing an elevated phosphorylation of tau. This would then lead to the dissociation of tau from microtubules so that microtubules become destabilized, axonal traffic would become impaired, and axons decay. The hyperphosphorylated tau could in turn aggregate into PHFs. The basic assumption of the hypothesis is therefore that the phosphorylation of tau would promote PHF aggregation. Some consequences are listed below:

(1) If tau were to be released from microtubules by "abnormal" phosphorylation during neurodegeneration, it should be phosphorylated at sites that decrease the affinity. The best candidates are S262 or S214 (targets of MARK or PKA) because both have a pronounced effect on tau's affinity to microtubules (*53*). This expectation is compatible with the observations because phosphorylated S262 and S214 are elevated in AD tau (*8*), and indeed phospho-S214 is recognized by one of the most specific antibodies against AD-tau (AT-100, ref *36*).

(2) The "abnormal" phosphorylation of tau in degenerating neurons should promote tau's aggregation into PHFs. This is clearly contrary to the observations described here.

(3) Specifically, the "abnormal" phosphorylation of tau should preferentially promote the interaction between the repeat domains because they form the backbone of PHF assembly in vivo and in vitro. Again this is contrary to the observations since the phosphorylation in the repeats inhibits PHF assembly.

(4) Since most sites considered to be diagnostic for "abnormal" phosphorylation are in SP or TP motifs in the domains flanking the repeats, proline-directed phosphorylation should strongly promote PHF assembly. This is also not observed since the SP or TP motifs have a weak influence, on both tau−microtubule interactions and PHF assembly.

(b) Structural Constraints and Modes of Phosphorylation. How does the phosphorylation of tau exert its effect on tau's interactions? From a structural point of view this question is difficult to address at present because the structure of tau is not known, and because tau is a highly flexible molecule capable of adopting many conformations (*54*). From a kinetic point of view we know that the assembly into PHFs must pass through several stages, (1) dimerization involving oxidation of Cys 322, (2) interactions with polyanions (presumably resulting in some conformational change), and (3) aggregation of dimers into filaments. We can therefore ask which of these levels is influenced by phosphorylation. Broadly speaking we can distinguish phosphorylation sites with strong or weak effects. The "strong" class includes the KXGS motifs and neighboring residues in the repeats (notably S262, S320, S324, S356) and S214 in the N-terminal flanking region. The "weak" sites are the SP or TP motifs in the flanking regions. The "strong" site S214 surprisingly does not perturb the initial dimerization (Figure 5c) and therefore must affect a later step in PHF assembly. On the other hand the "strong" sites in the KXGS motifs of the repeats clearly inhibit the dimerization of tau (Figure 5d). The sites S320 and S324 in the third repeat are especially interesting because they surround the C322 which forms the disulfide bridge between two monomers leading to dimerization of tau. We note that PKA phosphorylates S320 much better than MARK (at least in the repeat construct K19, Figure 7c,d); this could be the reason PKA inhibits the formation of PHFs better than MARK (Figure 7e,f,g). (Note that, in the absence of heparin, MARK phosphorylates the KXGS motifs of the repeats much more efficiently than PKA, especially S262 (*35*, *55*).

The repeat domain forms the core of the PHF (*32*, *52*), and therefore one may expect that the phosphorylation of this domain has an influence on PHF assembly, as observed. However, it is not obvious why a more distant residue such as S214 should have such a large influence, especially when considering the disordered and flexible nature of tau (*54*). A possible explanation is that tau adopts a conformation by which the N-terminal flanking domain is folded over the repeat domain, putting S214 in a position where its phosphorylation can block the addition of further subunits to PHFs (note that the dimerization of tau itself is not blocked, see Figure 5c). Supporting evidence for possible folded conformations of tau comes from the reactivity of tau antibodies (e.g., SMI-34, Alz-50, TG-3; refs *56*−*58*) or related studies (e.g., ref *59*), and this may explain why S214 forms part of a folded Alzheimer-specific epitope (antibody AT-100; refs *36*, *37*). The strong effect on PHF assembly is specific for S214 since other residues close to this site do not show it (e.g., S217 or S235; Figure 6).

One of the puzzles posed by the results is the observation that PHFs from AD brains are highly phosphorylated. The extensive phosphorylation at SP or TP motifs has been taken as evidence that this type of phosphorylation promotes PHF assembly. On the contrary, our results argue that these sites have a weak inhibitory effect on PHF assembly; they can be phosphorylated either before or after assembly, and their high extent of phosphorylation in AD tau could merely reflect the altered balance of kinases and phosphatases in degenerating neurons (*19*). Proline-directed kinases could be overactivated, and phosphatases could be suppressed or sterically blocked from attacking phosphorylation sites in the PHFs (note that Alzheimer PHFs cannot be dephosphorylated by phosphatases unless they are solubilized by denaturing agents; see refs *56*, *60*). On the other hand, the elevated phosphorylation of S214 and S262 in PHFs from AD brain (*8*, *40*) might appear contradictory since we show here that these sites are strongly inhibitory for PHF assembly. This is resolved when we consider the post-assembly phosphorylation of PHFs. The phosphopeptide patterns reveal a number of SP or TP sites, as well as S214, S262, and S356 (Figure 8). Apparently these sites are to some extent (∼30%) accessible for phosphorylation in the PHF structure, independently of their inhibitory effect on PHF formation. Another possibility is that, in AD, proteolytic fragments of tau representing the repeat domain are generated which can nucleate PHFs and whose assembly is less sensitive to phosphorylation (similar to K19, Figure 7, cf. ref *52*).

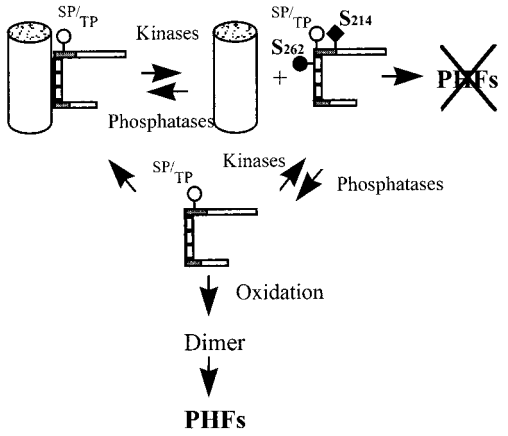

FIGURE 9: Model of the effects of phosphorylation on tau−microtubule interactions and PHF assembly. The phosphorylation state of tau is controlled by the balance between the various kinases (MAPK, GSK-3β, PKA, MARK...) and phosphatases (PP-2a, PP-2b...). Sites phosphorylated by proline-directed kinases (SP or TP in the regions flanking the repeats, symbolized by open circles) have only a moderate effect on tau−microtubule interactions and leave tau mostly attached to microtubules (top left). MARK and PKA detach tau from microtubules (top middle), mainly by phosphorylating KXGS motifs and neighboring sites in the repeats and S214 upstream of the repeats (filled circles and diamonds). The assembly of tau into PHFs is affected in the same way: proline-directed kinases have only a weak inhibitory effect and allow PHF assembly to proceed (reaction pathway center to bottom), and MARK and PKA are strongly inhibitory (top right).

The reactions are summarized in the diagram of Figure 9. Tau is shown with two types of phosphorylation sites, one with black symbols ("strong" sites regulating tau's interactions, i.e., KXGS motifs and S214), and the other with open symbols (SP or TP sites having little effect on interactions with microtubules, but important as targets of most diagnostic PHF antibodies). Tau that is not phosphorylated at "strong" sites can attach to microtubules and stabilize them (Figure 9, top left), but it can also aggregate into PHFs (bottom). Tau phosphorylated at the strong sites cannot interact with

microtubules (top middle), and it also resists incorporation into PHFs (top right). On the other hand, binding of tau to microtubules or assembly into PHFs is only weakly affected by the phosphorylation at SP or TP sites (open symbols). This means that we have to abandon the view that the "hyperphosphorylation" of tau observed in Alzheimer's disease primes tau for assembly into PHFs. On the contrary, phosphorylation (especially at "strong" sites) protects tau against assembly into PHFs. Therefore the excess phosphorylation of tau from Alzheimer PHFs must be seen in a different context: It is the consequence of PHF assembly rather than the cause of it. This phosphorylation could occur by tilting the balance between kinases and phosphatases toward phosphorylation, or by sterically preventing phosphatases from attacking PHF tau once it is assembled. This would be consistent with the observation that the enzymes regulating the "Alzheimer-like" phosphorylation are active in physiological conditions as well, and that their balance can be shifted as a result of stress, energy deprivation, or degeneration (*49*, *61*, *62*). It is interesting to note that phosphorylation of tau also stabilizes it against proteolytic degradation (*63*, *64*). This emphasizes the principle that the cell protects tau from malfunctioning by phosphorylating it.

In summary, the data force us to abandon one of the key assumptions relating the functions of tau to the PHF aggregation in AD. In hindsight, and from a physiological perspective, the "protection" of tau by phosphorylation is actually reasonable. If the cell needs to regulate the association between tau and microtubules by phosphorylation it would be counterproductive to detach tau from microtubules in a form that would favor some irreversible aggregation. On the contrary, the free tau should be in a form that keeps it ready for reattaching to microtubules, once it is dephosphorylated again. In this sense the "protective" phosphorylation (at S262, S214, or related sites) serves a dual role.

ACKNOWLEDGMENT

We are grateful to Katja Alm and Anja Konopatzki for expert technical assistance and to Peter Friedhoff and Qingyi Zheng-Fischhöfer for stimulating discussions. Antibody 12E8 was a generous gift of P. Seubert (Athena Neurosciences). This work forms part of the doctoral thesis of A.S. The project was supported by the Deutsche Forschungsgemeinschaft.

REFERENCES

1. Selkoe, D. (1998) *Trends in Cell Biol. 8*, 447−453.
2. Mandelkow, E.-M., and Mandelkow, E. (1998) *Trends Cell Biol. 8*, 425−427.
3. Braak, H., and Braak, E. (1991) *Acta Neuropathol. 82*, 239−259.
4. Gomez-Isla T., Hollister, R., West, H., Mui, S., Growdon, J. H., Petersen, R. C., Parisi, J. E., and Hyman, B. T. (1997) *Ann. Neurol. 41*, 17−24.
5. Butner, K. A., and Kirschner, M. W. (1991) *J. Cell Biol. 115*, 717−730.
6. Gustke, N., Trinczek, B., Biernat, J., Mandelkow, E.-M., and Mandelkow, E. (1994) *Biochemistry 33*, 9511−9522.
7. Grundke-Iqbal, I., Iqbal, K., Tung, Y., Quinlan, M., Wisniewski, H., and Binder, L. (1986) *Proc. Natl. Acad. Sci. U.S.A. 83*, 4913−4917.
8. Morishima-Kawashima, M., Hasegawa, M., Takio, K., Suzuki, M., Yoshida, H., Titani, K., and Ihara, Y. (1995) *J. Biol. Chem. 270*, 823−829.
9. Terry, R. D. (1996) *J. Neuropath. Exp. Neurol. 55*, 1023−1025.
10. Jarrett, J. T., and Lansbury, P. T. (1993) *Cell 73*, 1055−1058.
11. Wille, H., Drewes, G., Biernat, J., Mandelkow, E.-M., and Mandelkow, E. (1992) *J. Cell Biol. 118*, 573−584.
12. Schweers, O., Mandelkow, E.-M., Biernat, J., and Mandelkow, E. (1995) *Proc. Natl. Acad. Sci. U.S.A. 92*, 8463−8467.
13. Wilson, D., and Binder, L. I. (1997) *Am. J. Pathol. 150*, 2181−2195.
14. Perez, M., Valpuesta, J. M., Medina, M., Degarcini, E. M., and Avila, J. (1996) *J. Neurochem. 67*, 1183−1190.
15. Goedert, M., Jakes, R., Spillantini, M., Hasegawa, M., Smith, M., and Crowther, R. (1996) *Nature 383*, 550−553.
16. Kampers, T., Friedhoff, P., Biernat, J., Mandelkow, E.-M., and Mandelkow, E. (1996) *FEBS Lett. 399*, 344−349.
17. Hasegawa, M., Crowther, R. A., Jakes, B., and Goedert, M. (1997) *J. Biol. Chem. 272*, 33118−33124.
18. Friedhoff, P., Schneider, A., Mandelkow, E.-M., and Mandelkow, E. (1998) *Biochemistry 37*, 10223−10230.
19. Trojanowski, J., and Lee, V. M. Y. (1995) *FASEB J. 9*, 1570−1576.
20. Johnson, G., and Jenkins, S. (1996) *Alzheimer's Dis. Rev. 1*, 38−54.
21. Friedhoff, P., and Mandelkow, E. (1999) Tau Protein, in *Guidebook to the Cytoskeletal and Motor Proteins*, Kreis, T., Vale, R., Eds., Oxford University Press (in press).
22. Biernat, J., Gustke, N., Drewes, G., Mandelkow, E.-M., and Mandelkow, E. (1993) *Neuron 11*, 153−163.
23. Drewes, G., Ebneth, A., Preuss, U., Mandelkow, E.-M., and Mandelkow, E. (1997) *Cell 89*, 297−308.
24. Illenberger, S., Zheng-Fischhöfer, Q., Preuss, U., Stamer, K., Baumann, K., Trinczek, B., Biernat, J., Godemann, R., Mandelkow, E.-M., Godemann, R., and Mandelkow, E. (1998) *J. Biol. Cell 9*, 1495−1512.
25. Brandt, R., Lee, G., Teplow, D., Shalloway, D., and Abdelghany, M. (1994) *J. Biol. Chem. 269*, 11776−11782.
26. Jenkins, S. M., and Johnson, G. V. W. (1997) *Brain Res. 767*, 305−313.
27. Goedert, M., Spillantini, M., Potier, M., Ulrich, J., and Crowther, R. (1989) *EMBO J. 8*, 393−399.
28. Song, J. S., and Yang, S. D. (1995) *J. Protein Chem. 14*, 95−105.
29. Moreno, F. J., Munoz-Montano, J. R., and Avila, J. (1996) *Mol. Cell. Biochem. 165*, 47−54.
30. Boyle, W. J., van der Geer, P., and Hunter, T. (1991) *Methods Enzymol. 201*, 110−149.
31. Illenberger, S., Drewes, G., Trinczek, B., Biernat, J., Meyer, H. E., Olmsted, J. B., Mandelkow, E. M., and Mandelkow, E. (1996) *Biol. Chem. 271*, 10834−10843.
32. Wischik, C., Novak, M., Thogersen, H., Edwards, P., Runswick, M., Jakes, R., Walker, J., Milstein, C., Roth, M., and Klug, A. (1988) *Proc. Natl. Acad. Sci. U.S.A. 85*, 4506−4510.
33. Bancher, C., Grundke-Iqbal, I., Iqbal, K., Fried, V., Smith, H., and Wisniewski, H. (1991) *Brain Res. 539*, 11−18.
34. Braak, E., Braak, H., and Mandelkow, E.-M. (1994) *Acta Neuropath. 87*, 554−567.
35. Drewes, G., Trinczek, B., Illenberger, S., Biernat, J., Schmitt-Ulms, G., Meyer, H. E., Mandelkow, E. M., and Mandelkow, E. (1995) *J. Biol. Chem. 270*, 7679−7688.
36. Zheng-Fischhöfer, Q., Biernat, J., Mandelkow, E.-M., Illenberger, S., Godemann, R., and Mandelkow, E. (1998) *Eur. J. Biochem. 252*, 542−552.
37. Hoffmann, R., Lee, V. M. Y., Leight, S., Varga, I., and Otvos, L. (1997) *Biochemistry 36*, 8114−8124.
38. Gross, U. (1996) Ph.D. Thesis, University of Hamburg.
39. Dickson, D., Ksiezak-Reding, H., Liu, W., Davies, P., Crowe, A., and Yen, S. H. (1992) *Acta Neuropath. 84*, 596−605.
40. Seubert, P., Mawaldewan, M., Barbour, R., Jakes, R., Goedert, M., Johnson, G. V. W., Litersky, J., Schenk, D., Lieberburg, I., Trojanowski, J., and Lee, V. M. Y. (1995) *J. Biol. Chem. 270*, 18917−18922.
41. Arriagada, P. V., Growdon, J. H., Hedley-Whyte, E., and Hyman, B. T. (1992) *Neurology 42*, 631−639.
42. Kosik, K. S. (1993) *Brain Pathol. 3*, 39−43.

43. Mandelkow, E.-M., Biernat, J., Drewes, G., Gustke, N., Trinczek, B., and Mandelkow, E. (1995) *Neurobiol. Aging 16*, 355−362.
44. Vigo-Pelfrey, C., Seubert, P., Barbour, R., Blomquist, C., Lee, M., Lee, D., Coria, F., Chang, L., Miller, B., Lieberburg, I., and Schenk, D. (1995) *Neurology 45*, 788−793.
45. Hanemaaijer, R., and Ginzburg, I. (1991) *J. Neurosci. Res. 30*, 163−171.
46. Kosik, K. S., and McConlogue, L. (1994) *Cell Motil. Cytoskeleton 28*, 195−198.
47. Ebneth, A., Godemann, R., Stamer, K., Illenberger, S., Trinczek, B., Mandelkow, E.-M., and Mandelkow, E. (1998) *J. Cell Biol. 143*, 777−794.
48. Ksiezak-Reding, H., Liu, W. K., and Yen, S. H. (1992) *Brain Res. 597*, 209−219.
49. Matsuo, E. S., Shin, R. W., Billingsley, M. L., Vandevoorde, A., Oconnor, M., Trojanowski, J. Q., and Lee, V. M. Y. (1994) *Neuron 13*, 989−1002.
50. Cleveland, D. W., Hwo, S.-Y., and Kirschner, M. W. (1977) *J. Mol. Biol. 116*, 227−247.
51. Lee, G., Cowan, N., and Kirschner, M. (1988) *Science 239*, 285−288.
52. Novak, M., Kabat, J., and Wischik, C. M. (1993) *EMBO J. 12*, 365−370.
53. Drewes, G., Ebneth, A., and Mandelkow, E.-M. (1998) *Trends Biochem. Sci. 23*, 307−311.
54. Schweers, O., Schönbrunn, E., Marx, A., and Mandelkow, E. (1994) *J. Biol. Chem. 269*, 24290−24297.
55. Scott, C., Spreen, R., Herman, J., Chow, F., Davison, M., Young, J., and Caputo, C. (1993) *J. Biol. Chem. 268*, 1166−1173.
56. Lichtenberg-Kraag, B., Mandelkow, E.-M., Biernat, J., Steiner, B., Schröter, C., Gustke, N., Meyer, H.E., and Mandelkow, E. (1992) *Proc. Natl. Acad. Sci. U.S.A. 89*, 5384−5388.
57. Carmel, G., Mager, E. M., Binder, L. I., and Kuret, J. (1996) *J. Biol. Chem. 271*, 32789−32795.
58. Jicha, G. A., Bowser, R., Kazam, I. G., and Davies, P. (1997) *J. Neurosci. Res. 48*, 128−132.
59. Goode, B., Denis, P., Panda, D., Radeke, M., Miller, H., Wilson, L., and Feinstein, S. (1997) *Mol. Biol. Cell 8*, 353−365.
60. Greenberg, S. G., Davies, P., Schein, J. D., and Binder, L. I. (1992) *J. Biol. Chem. 267*, 564−569.
61. Papasozomenos, S., and Su, Y. (1995) *J. Neurochem. 65*, 396−406.
62. Song, J., Combs, C., Pilcher, W., Song, L., Utal, A., and Coleman, P. (1997) *Neurobiol. Aging 18*, 475−481.
63. Litersky, J. M., and Johnson, G. V. W. (1992) *J. Biol. Chem. 267*, 1563−1568.
64. Mercken, M., Grynspan, F., and Nixon, R. A. (1995) *FEBS Lett. 368*, 10−14.
65. Drechsel, D. N., Hyman, A. A., Cobb, M. H., and Kirschner, M. W. (1992) *Mol. Biol. Cell 3*, 1141−1154.
66. Hasegawa, M., Morishima-Kawashima, M., Takio, K., Suzuki, M., Titani, K., and Ihara, Y. (1992) *J. Biol. Chem. 267*, 17047−17054.
67. Litersky, J., Johnson, G., Jakes, R., Goedert, M., Lee, M., and Seubert, P. (1996) *Biochem. J. 316*, 655−660.

BI981874P